

Arterial Wall Diameter and Viscoelasticity Variability

LG Gamero^{1,3}, RL Armentano¹, J Levenson²

¹Favaloro University, Buenos Aires, Argentina

²Hôpital Broussais, CMPVC, INSERM, Paris, France

³Facultad de Ingeniería, Entre Ríos University, Argentina

Abstract

The aim of this study was to evaluate and characterize arterial diameter and arterial wall viscoelastic variability. An animal study was performed on seven sheep instrumented in the brachycephalic artery. ECG, arterial diameter and pressure waveforms were simultaneously measured. Four different hemodynamic conditions were considered: 1) under anesthesia, 2) conscious steady state, 3) vascular smooth muscle (VSM) activation and 4) VSM relaxation. A system modeling identification approach was applied in order to estimate viscoelastic indexes. The linear autoregressive with exogenous input model (ARX) was applied to the single beat pressure-diameter data to assess the arterial system dynamics. The elastic and viscous indexes were derived from the identified ARX model. Arterial pressure and diameter, heart rate and viscoelastic indexes variability analysis were performed in the time and frequency domains. While systolic pressure and arterial diameter oscillation show a similar pattern to heart rate at all frequency bands in control condition, wall viscosity variability does not match with these parameters ($p < 0.05$). Compared with control condition, arterial diameter variability was lower during anesthesia and higher during VSM relaxation ($p < 0.05$). The elastic index variability was lower during anesthesia and VSM relaxation and higher during VSM activation. The different behavior of arterial wall viscoelasticity suggests that intrinsic mechanisms related with vascular tone and vasomotion might be involved in the oscillatory pattern of the arterial wall.

1. Introduction

Several pathophysiological conditions affecting the cardiovascular system are characterized by a dysfunction of the viscoelastic properties of large arteries. These alterations have pathophysiological relevance because arterial wall properties play a key role in cardiovascular homeostatic control by modulating a number of important parameters, such as arterial impedance, cardiac after load

and myocardial oxygen consumption.

The arterial wall can be considered as a viscoelastic material whose mechanical properties determine the artery buffering function [1, 2]. Arteries often exhibit spontaneous rhythmic activity, which is manifested by low frequency oscillations in a phenomenon termed vasomotion. This condition is predominant in small arteries and microcirculation, but recently it has been shown to exist in large muscular arteries [3]. In large arteries, the physiological significance of this oscillation and its relationship with myogenic and smooth muscle activity remain obscure [4, 5]. Diameter oscillation results from blood pressure and also from local properties of the arterial wall, such as viscoelasticity and endothelial function (flow-mediated dilation).

The aim of this study was to evaluate simultaneously the oscillations in heart rate, blood pressure, arterial diameter and arterial wall viscoelasticity in different hemodynamic conditions. For this purpose, an animal study was performed on sheep. We analyzed the variability of heart rate, brachiocephalic arterial pressure and diameter. Beat to beat arterial wall viscoelasticity was estimated using a viscoelastic model. The same variability analysis was performed in this time series to clarify the contribution of wall viscoelasticity to the arterial wall oscillatory patterns.

2. Methods

2.1. Surgical preparation

Seven male sheep were instrumented in the brachiocephalic artery in order to measure ECG, instantaneous arterial diameter and pressure. Anesthesia was induced with intravenous thiopental sodium (20 mg kg^{-1}) and, after intubation, maintained with 2% enflurane carried in pure oxygen (4 l min^{-1}) through a Bain tube connected to a Bird Mark VIII respirator. A sterile thoracotomy was made at the left fifth intercostal space. A pressure microtransducer (Konigsberg) and a fluid-filled polyvinyl chloride catheter for later calibration of the microtransducer were implanted in the brachycephalic artery. A pair of ultrasonic crystals (5

MHz, 4 mm diameter) was sutured on the adventitia of the artery, after minimal dissection, to measure external arterial diameter. The transit time of the ultrasonic signal (1580 m s^{-1}) was converted into distance using a sonomicrometer (Triton Technology Inc.). A polyvinyl chloride catheter (2.3 mm OD) was advanced through the left mammary vein to lie in the superior vena cava or right atrium for drug administration. Before repairing the thoracotomy, all cables and catheters were tunneled subcutaneously to emerge at the interscapular space. The experiments were performed in accordance with the *Guide for the Care and Use of Laboratory Animals* [6].

2.2. Experimental protocol

Experiments and data collection started on the seventh postoperative day. One lead ECG, arterial pressure and diameter were measured simultaneously in four different hemodynamic conditions: 1) under anesthesia (ANE), 2) in control unsedated condition (CTR), 3) under smooth muscle activation (PHN)¹ and 4) under smooth muscle relaxation (NPS)². Conditions 2–4 were fulfilled with the sheep resting quietly on its right side in conscious unsedated state. Signals were digitized using a 12 bit A/D converter and sampled at 250 Hz.

An automatic procedure was developed for QRS detection, arterial pressure and diameter waveform analysis [7]. Beat to beat RR interval, systolic and diastolic arterial diameter and pressure were obtained for each experimental condition. Figure 1 shows an example of the signals: ECG, arterial pressure and diameter during conscious unsedated condition.

Berger's interpolation method [8] with a sampling frequency of 2 Hz was applied to the signals. Power spectral analysis was performed on the time series to obtain very low frequency (VLFN), low frequency (LFN) and high frequency (HFN) components, normalized with total power.

2.3. System modeling

The arterial pressure-diameter (x - y) relationship can be modeled by the following continuous-time linear differential equation:

$$\sum_{i=0}^n a_i \frac{d^i x}{dt^i} = y(t) + \sum_{j=1}^m b_j \frac{d^j y}{dt^j}, \quad (1)$$

where the coefficients $\{a_i, i = 0, \dots, n\}$ and $\{b_j, j = 1, \dots, m\}$ define the material's viscoelastic properties and the model order is represented by n and m .

¹Phenylephrine administration ($5 \text{ g kg}^{-1} \text{ min}^{-1}$), infused in parallel with the dextrose drip).

²Nitroprusside sodium.

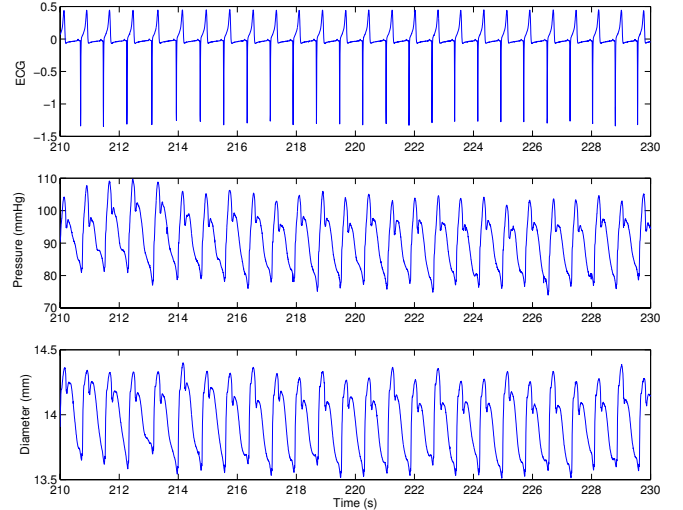


Figure 1. Example of ECG, arterial pressure and diameter signals during control condition.

The arterial pressure-diameter relation is non-linear, with less change in diameter with increasing pressure [9, 3, 10]. Arterial wall pressure-diameter hysteresis loop mainly involves three properties: the elastic index ($k_E=a_0$), viscous index ($k_\eta=a_1$) and inertial index ($k_M=a_2$) [10, 11, 12].

The description of the viscoelastic properties as represented in (1) is general when the material is linear and time invariant, or when only very small excursions from a working point are considered [13]. Since the arterial wall is not linear, we considered the measured data about a working point, which can be established to be around the mean arterial diameter and pressure measurements [7].

In order to estimate the parameters of (1), a discrete-model system identification approach is proposed. A linear parametric AutoRegressive with eXogenous input (ARX) model is described by [14]:

$$\hat{y}(t|\theta) = \theta^T \varphi(t), \quad (2)$$

where $\varphi = [y(t-1), \dots, y(t-n), x(t), \dots, x(t-m)]^T$ is the input vector and $\theta \in \mathbb{R}^{m+n+1}$ is the parameter vector to be estimated on the basis that input-output data (pressure-diameter) $y(t)$ and $\varphi(t, \theta)$ for $\{t = 1, \dots, N\}$ are known. It is important to notice that the parameters from (1) can be related to the ARX parameters through a complex mapping. The inverse bilinear mapping from z to s plane was used to reach this task [15]. In this study, the optimal order model was the one that minimized the Akaike's Information Criterion [16] defined by:

$$AIC(N_p) = N \ln(\sigma_e^2) + 2N_p, \quad (3)$$

where N_p is the number of parameters, N is the number of

data samples and σ_e^2 is the residual variance

$$\sigma_e^2 = \frac{1}{N-1-p} \sum_{t=d+1}^N e(t)^2, \quad (4)$$

where $d = \max\{n, m\}$. Other criteria can be considered but the AIC is a good compromise between the number of parameters and the residual variance [14]. The general third order model was determined as the mean best order model.

To assess the arterial wall viscoelasticity, the ARX model was applied in a beat-to-beat basis to the input-output data. Model parameters were computed using the least squares algorithm [14]. After this procedure, the beat-to-beat viscoelasticity indexes were interpolated and analyzed in the frequency domain in the same way as the other signals.

All measurements and calculated values are expressed as mean \pm SD. The presence of significant differences in the estimated parameters was assessed using ANOVA and Bonferroni post-hoc tests. Smooth muscle activation and relaxation parameters were compared with that corresponding to control condition by using a paired t -test. Values of t with $p < 0.05$ were considered statistically significant.

3. Results and conclusion

Figure 2 shows an example of the results of the automatic beat detection procedure. Beat to beat RR interval, systolic and diastolic pressure and diameter are presented during an experiment of phenylephrine infusion. The first segment of the data corresponds to the control condition, and after 3 min PHN was infused (see figure 2a). The effect of PHN infusion can be summarized as an increase in pressure, diameter and RR (decrease in heart rate).

After beat fiducial points detection, parameter estimation (viscous and elastic indexes) was performed on a beat to beat basis. The time evolution of the arterial indexes is presented in figure 3. Arterial pressure and diameter, heart rate and viscoelastic indexes variability analysis were performed in the time and frequency domains in the VLF, LF and HF frequency bands. Table 1 shows heart rate, blood pressure, arterial diameter and arterial wall viscosity normalized power at VLF, LF and HF frequency bands during the control condition. Systolic pressure and arterial diameter oscillations show a similar pattern compared to heart rate at all frequency bands. A significant difference was found comparing these variables with arterial wall viscosity variability.

Table 2 shows a summary of the standard deviation of consecutive normal beats (SDNN) for the 4 conditions. Comparing against the control condition, arterial diameter variability was lower during anesthesia and higher during

VSM relaxation ($p < 0.05$). The elastic index variability was lower during anesthesia and VSM relaxation and higher during VSM activation.

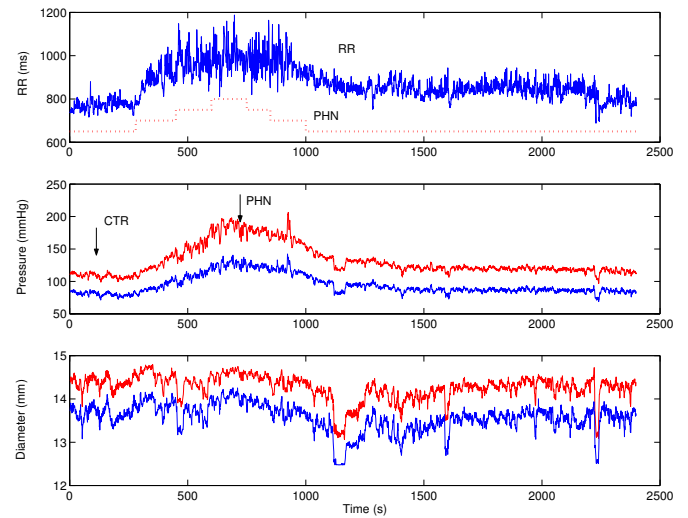


Figure 2. Beat to beat a) RR interval (solid line) and PHN dose infusion (dot line), b) systolic and diastolic pressure and c) systolic and diastolic diameter during conscious CTR and PHN conditions.

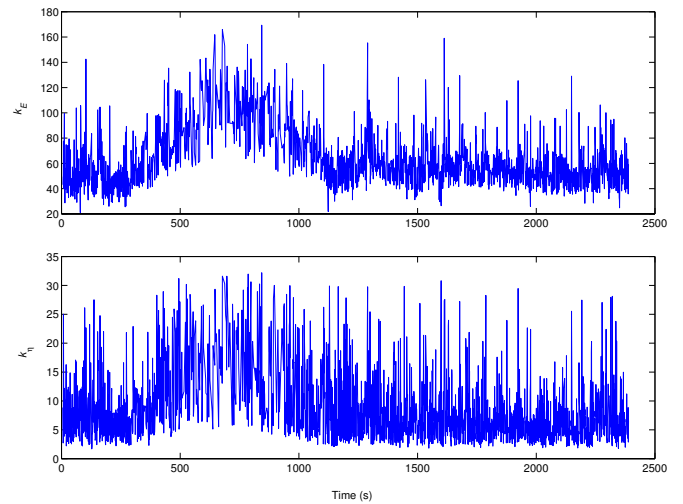


Figure 3. Elastic and viscous indexes estimation based on the ARX single beat identification approach during PHN infusion.

In conclusion, the intrinsic oscillation of heart rate, pressure, arterial wall diameter and viscoelastic properties was presented in this study. The different behavior of arterial viscoelasticity suggests that intrinsic mechanisms related with vascular tone and vasomotion might be involved in the oscillatory pattern of the arterial wall. An understanding of the pressure-diameter oscillation and the intrinsic properties of the arterial wall will enhance our basic knowledge of the functional properties of large

arteries, and therefore we believe that the relationship between local and central regulatory mechanisms merits further investigation.

Table 1. Power spectral analysis of heart rate (HR), arterial blood pressure (BP), arterial diameter (D) and arterial wall viscous index (k_η) in control condition. Frequency bands are normalized to total power. ANOVA, Bonferroni post hoc test ($n=7$), $\dagger p<0.05$ comparing k_η versus HR, BP and D.

	VLF/TP	LF/TP	HF/TP
HR	0.74±0.10	0.18±0.06	0.08±0.06
BP	0.84±0.09	0.13±0.07	0.03±0.01
D	0.78±0.11	0.16±0.07	0.06±0.03
k_η	0.41±0.11 \dagger	0.33±0.07 \dagger	0.26±0.08 \dagger

Table 2. Standard deviation of HR, BP, D, k_η and k_E in CTR, ANE, PHN and NPS conditions. Unpaired t -Student's test, ($n=7$), $\dagger p<0.05$ comparing HR, BP, D, k_η and k_E versus CTR.

	CTR	ANE	PHN	NPS
RR	45±27	17±14 \dagger	63±22	50±22
P	5.2±3.2	3.2±1.1	13.1±4.10 \dagger	6.4±2.5
D	.14±.07	.11±.03 \dagger	.18±.09	.25±.13 \dagger
k_E	9.8±6.1	3.1±2.9 \dagger	18.2±14.7 \dagger	3.6±1.8 \dagger
k_η	3.7±3.3	0.6±0.4 \dagger	4.4±3.1	.41±.33 \dagger

References

[1] Westerhof N, Noordegraaf A. Arterial viscoelasticity: a generalized model. Effect on input impedance and wave travel in the systemic tree. *J of Biomech* 1970;3:357–379.

[2] O'Rourke M. Second workshop on structure and function of large arteries: Part I. Mechanical principles in arterial disease. *Hypertension* 1995;26(1):2–9.

[3] Hayashi K. Experimental approaches on measuring the mechanical properties and constitutive laws of arterial walls. *J of Biomech Eng* 1993;115:481–488.

[4] Stergiopoulos N, Porret CA, de Brouwer S, Meister JJ.

Arterial vasomotion: effect of flow and evidence of nonlinear dynamics. *Am J Physiol* 1998;274:H1858–H1864.

[5] Tardy Y, Meister JJ, Perret F, Brunner HR, Arditì M. Non-invasive estimate of the mechanical properties of peripheral arteries from ultrasonic and photoplethysmographic measurements. *Clin Phys Physiol Meas* 1991;12(1):39–54.

[6] National Institutes of Health. Guide for the care and use of laboratory animals. Technical Report 85-23, NIH, Washington, DC, 1985.

[7] Gamero LG. Identificación y Caracterización de la Dinámica Cardiovascular. Ph.D. thesis, Facultad de Ingeniería, Universidad de Buenos Aires, 2002.

[8] Berger RD, Akselrod S, Gordon D, Cohen J. An efficient algorithm for spectral analysis of heart rate variability. *IEEE Transaction on Biomedical Engineering* 1986;33:900–904.

[9] Fung YC. Biomechanics. Mechanical Properties of Living Tissues. New York: Springer-Verlag, 1981.

[10] Armentano RL, Barra JG, Levenson J, Simon A, Pichel RH. Arterial wall mechanics in conscious dogs. *Circ Research* 1995;76:468–478.

[11] Gamero L, Armentano R, Barra J, Levenson J, Pichel R. Non-invasive single beat modeling of human carotid properties in hypertension. In *Computers in Cardiology*, volume 24. Los Alamitos: IEEE Computer Society Press, 1997; 449–452.

[12] Gamero L, Armentano R, Barra J, Simon A, Levenson J. Identification of arterial wall dynamics in conscious dogs. *Experimental Physiology* 2001;86(4):519–528.

[13] Gow BS, Taylor MG. Measurements of viscoelastic properties of arteries in the living dog. *Circ Research* 1968; 23:111–122.

[14] Ljung L. System Identification. Theory for the User. 2nd ed. Upper Saddle River, N. J.: PTR Prentice Hall, 1999.

[15] Lam HY. Analog and Digital Filters: Design and Realization. Englewood Cliffs, New Jersey: Prentice Hall, 1980.

[16] Sakamoto M, Ishiguro M, Kitagawa G. Akaike information criterion statistic. Hingham, MA: D. Reidel Publ. Co., 1986; 184–194.

Address for correspondence:

Lucas G. Gamero, Ph.D.
Zargis Medical Corp.
755 College Road East
Princeton, NJ 08540
Tel: (609) 734–6576
lgamero@zargis.com